EURAMET TC Project
Final Report

Project Title

R-134a leak comparison in atmospheric pressure

Coordinator, Institute, Country

Frédéric BOINEAU, LNE (France)

EURAMET Registration No.

1115

Subject Field

Mass and Related Quantities

KCDB Identifier

--

Date

2022-02-03

EURAMET e.V., Bundesallee 100, 38116 Braunschweig, Germany
Phone: +49 531 592 1960 Fax: +49 531 592 1969 E-mail: secretariat@euramet.org
www.euramet.org

Final Report - Project EURAMET n°1115
R-134a leak comparison in atmospheric pressure

Frédéric BOINEAU, Karl JOUSTEN, Dominik PRAZAK

Version: 03/02/2022[1]

[1] All the dates in the document are reported as dd/mm/yyyy

CONTENT

1. Introduction

Regarding the council Decision 2002/358/CE, made on April 25th 2002, concerning the approval on behalf of the European Community of the Kyoto Protocol, the European Union and its members had to reduce emissions of greenhouse gases, like R-134a, during the period 2008-2012. The European regulation n°842/2006 of May 17th 2006 relating to the refrigerant greenhouse gases defines the duties of the owners of such equipment. Thus, the owners of equipment confining more than 3 kg of refrigerant fluids must control periodically the tightness of their equipment, using for instance portable refrigerant leak detectors. The detection limit of refrigerant detectors must be checked according to the European standard EN 14624. In this standard, the performance of a detector is tested in different configurations by means of refrigerant leak artefacts with nominal mass flow rates between 1 and 50 g/a[(2)]. In Europe, some standards are suitable to calibrate R-134a leak flow rates. Therefore, it was decided to perform a comparison of R-134a leak artefacts that flow at the atmosphere to test the calibration measurement capabilities and to compare the standards.

A key comparison of helium rates flowing into vacuum was carried out between 2007 and 2013 [1]. The specificity of the present comparison is that the leak rate is referred to atmosphere. It was initiated in 2009 and the participants were the following national metrology institutes (NMIs): INRIM, LNE, PTB and CMI. LNE volunteered to be the pilot laboratory. The comparison was performed with two leak artefacts of R-134a: FCR-model from the manufacturer SAPRE (France), with respective nominal flow rate of 1.3 g/a ($4 \cdot 10^{-10}$ mol/s) and 3.6 g/a ($1 \cdot 10^{-9}$ mol/s).

2. Transfer standards and quantity to be determined

The two R-134a leak artefacts (L1 and L2) used as transfer standards are described in Table 1. They were equipped with a flange DN40 ISO KF (Figure 1).

Each artefact consists in a reservoir containing the refrigerant species in both liquid and gas phases. The gas phase is at the absolute saturation vapour pressure of approximately 570 kPa (at 20 °C). The membrane at the exit of the reservoir (the leak element) is crossed by the refrigerant gas, which allows a stable leak flow rate to be established. The presence of the two phases in the reservoir ensures a stable pressure as long as a stable temperature is maintained. Consequently the first identified influence parameter is the temperature. During the

[2] g/a: gram per year, 1 year is taken equal to 31 536 000 s.

characterisation of the artefacts, it was stated that the leak rate was also influenced by the downstream pressure variation.

Table 1. Types and dimensions of the transfer standard leaks (both R-134a leak artefacts)

Leak	**Manufacturer**	**Model**	**SN**	**Approx. value in mol/s**	**Length in mm**	**Diameter in mm**
L1	SAPRE	FCR3	435	$1 \cdot 10^{-9}$	140.5	19.9
L2	SAPRE	FCR1	436	$4 \cdot 10^{-10}$	140.5	19.9

Figure 1. Photograph of the two transfer standards.

Similarly to [1], the measurand to be determined is the molar flow rate q_ν of R-134a flowing out of the transfer leak artefacts, with $\Delta\nu$ the number of moles of R-134a exiting out of the leak during the time Δt:

$$q_\nu = \frac{\Delta\nu}{\Delta t}, \tag{1}$$

The target temperature was (20.0 ± 0.3) °C. When possible, for a better accuracy, all the measured values at a temperature different from 20.0 °C are recalculated for 20.0 °C exactly, by applying the determined temperature coefficient.

It is well known for helium leak artefacts with a reservoir that the flow rate decreases with time on the long term period as it was emphasized during the key comparison CCM.P-K12 [1]. The reservoir of L1 and L2 contains both liquid and gaseous phase of R-134a equilibrated at the saturation vapour pressure. From LNE's observations on the calibration history for this leak artefact of this type, there is not a clear trend of flow's decreasing with time thus a random variation can be assumed.

Leaks calibration were performed twice as a minimum by each laboratory (one calibration a week over two weeks). The scatter of the data enables the pilot laboratory to evaluate the random uncertainty due to the short term stability.

It was also observed from the pilot measurements and additional measurements at PTB, that the measured molar flow rate slightly varies with the downstream pressure p_d (which is more or less the atmospheric pressure value).

Finally, the quantity studied for the comparison is:

$$q(\theta_0; p_{d0}) = \frac{\Delta v}{\Delta t}, \quad (2)$$

At the temperature θ_0 = 20.0 °C and the downstream pressure p_{d0} = 100 kPa.

3. Participating laboratories and their measurement systems

Table 2 lists, in the alphabetical order, the four laboratories which participated in this comparison with, in the second column, the standards used for the calibration of the transfer standards. The third column indicates whether the standard is considered as primary or secondary; the fourth column gives the method and the last column lists whether the standard is independent or traceable to another NMI.

Table 2. List of participants in alphabetic order and associated standards and methods.

Laboratory	Standard used	Type	Method	Independent
CMI Czech Metrological Institute Czech Republic	Mettler-Toledo AT10005 & DH-Instruments GFS	primary	Mass variation	Yes
INRIM Istituto Nazionale di Ricerca Metrologica Italy	Constant pressure flowmeter	primary	Volume variation at constant pressure	Yes
LNE Laboratoire National de Métrologie et d'Essais France (Pilot Laboratory)	Concentration rise method in a constant volume	primary	Concentration variation of R-134a	Yes
PTB Physikalisch-Technische Bundesanstalt Germany	Constant-pressure method in a variable volume	primary	Constant pressure	Yes

INRIM and PTB used a so-called constant pressure flowmeter which aims at measuring the volume variation with time $\Delta V/\Delta t$ that is necessary to maintain the internal pressure of a vessel, to which the leak is connected, at a constant value of p_0. Assuming a constant temperature T during the measurement, the determined throughput q_{pV} is given by the equation:

$$q_{pV} = p_0 \frac{\Delta V}{\Delta t}, \text{ at temperature } T. \quad (3)$$

The molar flow rate q_v is deduced from the ideal gas law:

$$q_v = \frac{q_{pV}}{RT}, \quad (4)$$

R = 8.3145 J mol^{-1} K^{-1} being the molar gas constant.

The reference standard of CMI delivers a mass flow rate of R-134a q_m. The corresponding molar flow rate is then given by the following equation:

$$q_v = \frac{q_m}{M}, \quad (5)$$

where M = 102.03 g·mol^{-1} is the molar mass of the gas R-134a.

The LNE reference standard delivers a concentration variation with time that is converted into a mass flow rate using the ideal gas law (cf. Equation (8)) for practical purposes.

3.1. CMI

A weighing method was used. It consists of comparing a standard mass (1 kg mass of class E1) and the mass of the transfer standard leak which was put into a brass base to ensure its stability and which was adjusted as near as possible to 1 kg with the help of the fractional masses, see Figure 2 [2-4]. The mass deviation between the two systems was determined with the following standard: a Mettler mass comparator, type AT10005. Its range is 10 kg, resolution 1·10^{-8} kg and best repeatability 3·10^{-8} kg (typical 5·10^{-8} kg). It has a relatively high range for this purpose, but enough space to place a leak. Its photograph with a loaded transfer standard is in Figure 3.

Figure 2. A transfer standard on its base with the trim masses added.

Figure 3. Photograph of the utilized mass comparator.

The mass deviation difference was obtained from three weighings: the first weighing of the standard mass, the weighing of the measured mass and the second weighing of the standard

mass. The variation in time of this mass deviation was observed in a time interval between 32 and 48 hours. The value of the leak (mass flow rate) is given by the mass change δ_m during time interval δ_t:

$$q_m = \frac{\delta_m}{\delta_t}. \quad (6)$$

The temperature of the leak could neither be regulated nor measured: the indicated temperature is the temperature of the laboratory room. However, temperature was recorded both in the room and the comparator chamber: a correction of +0.090 °C was applied to the temperature laboratory measurements. Besides, because of the dimensions of the comparator, the leak could not be installed horizontally: except during measurements on the mass comparator, both leaks were always stored in horizontal position. None of the leaks was connected to any vacuum or oily system at any time or had its flange closed.

Type B uncertainty contributions comes from the comparator resolution, the comparator instability (determined by comparing the standard mass with itself), the neglected buoyancy corrections, the resolution of the time measurements (the mass is weighed - reading integrated - during 10 s, with an uncertainty mainly due to the resolution of 1 s). Some measurements of both leaks were performed at the dynamic gravimetric flow system (DH-Instruments GFS). However, the results were not satisfactory enough and they are not included in this report.

3.2. INRIM

INRIM used a comparison method with a primary flowmeter (see Figure 4) based on constant pressure- changing volume in order to measure small gas flow of R134a referred to atmosphere (ambient pressure).

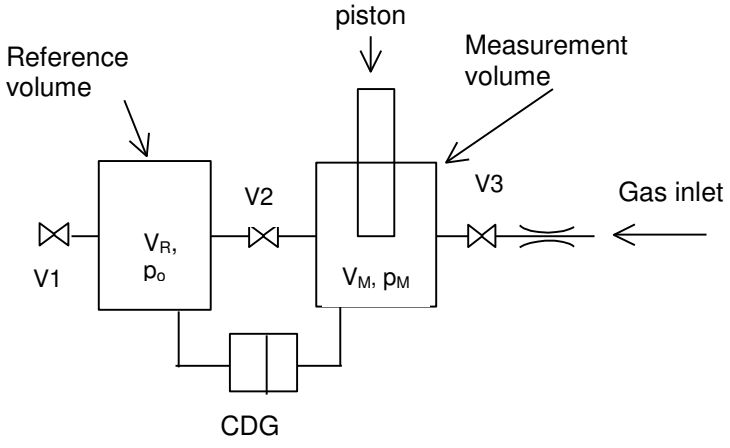

Figure 4. Scheme of a primary flow meter used to measure gas flows supplied through the leak in calibration

The operating principle is the following: the increasing pressure caused by the gas flow is compensated by a changing volume.

The molar flow generated by the flowmeter is calculated as:

$$q = p_0 \cdot \pi \cdot \frac{d^2}{4} \cdot \frac{dL}{dt} \cdot \frac{1}{RT_q}, \quad (7)$$

where p_0 is the reference pressure in the flowmeter (atmospheric pressure), d and L are respectively the diameter and the displacement of the piston, T_q is the mean temperature of the flowmeter and R = 8.3145 J·mol^{-1}·K^{-1} is the ideal gas constant.

The atmospheric pressure was measured with a barometer referred to INRIM mercury manometer, the temperature measurements are traceable to ITS90. The temperature of the laboratory is regulated at (20.0 ± 0.5) °C by an active control. The gas measurement chamber is surrounded by an annular aluminum jacket and it is in direct thermal contact with an aluminum slab of 3 cm thickness. The connection tubes and valves are also connected to a slab by copper spacers. Inside the slab the water circulates into channels and its temperature is controlled by an external refrigerated bath (from -35 °C to 200 °C). The temperature variation is less than 0.02 °C. The temperature stability is better than 0.004 °C in the time (less than 10 minutes) required to have a pressure rise when a flow of 10^{-6} Pa m^3/s is measured. The leak has been stabilized at least 24 hours before beginning the measurements in order to reach the equilibrium in permeation rate and temperature.

The relative standard uncertainty of INRIM flowmeter:

$U(q)/q$ = 1.6 % – 3 % $q = 5 \cdot 10^{-4}$ Pa m^3/s - $5 \cdot 10^{-5}$ Pa m^3/s

$U(q)/q$ = 3 % – 10 % $q = 5 \cdot 10^{-5}$ Pa m^3/s - $1 \cdot 10^{-6}$ Pa m^3/s

3.3. LNE

LNE used an accumulation method based on infrared detection [5]. The standard is based on the ability of the photo-acoustic spectrometer (PAS) to distinguish the concentration of the gas species absorbing IR light in a mixture containing gases that do not absorb IR light. It consists in measuring a concentration rise inside an accumulation volume that is also measured. The mass flow rate can then be calculated using:

$$\frac{\partial m}{\partial t} = \frac{M}{R} \cdot V \cdot \frac{\partial\left({}^{pC}/_{T}\right)}{\partial t}, \quad (8)$$

where m, T, p, M, R, V and C are respectively the mass, the temperature, the pressure, the molar mass of the gas, the molar gas constant, the accumulation volume and the accumulated concentration inside the volume.

To control the temperature of the transfer leaks, a thermo-regulated bath filled with water and equipped with an external circulation was used. A plastic tubing of 6 mm inner diameter, connected to the external circulation of the bath, surrounds the leak and regulates its temperature at 20 °C. A calibrated Pt100 sensor was attached to the reservoir of the transfer leak. The leak's temperature is assumed to be the Pt100 sensor's temperature. The instability of temperature (given by standard deviation of the mean) measured with the sensor was lower than 10 mK over 3 days.

Type B uncertainty contribution mainly comes from the spectrometer calibration and stability, the calibration of the accumulation volume and the residual leak flow rate inside the system.

3.4. PTB

PTB used the constant pressure method. The quantity to be determined is the number of gas molecules flowing out of the standard leak per time. An increasing number of molecules in an enclosed volume will increase the pressure in the same volume.

Two separate volumes are formed (Figure 5): the working volume V_{wv} and the reference volume V_{ref}. Any pressure difference between these two volumes is measured by the differential CDG. The gas flow from the test leak increases the pressure in V_{wv} continuously. After a defined increase, the volume is increased by ΔV by moving a sealed needle out of V_{wv} in order to reduce the pressure to its initial value. The time Δt it takes to reach the threshold is measured. The molar flow is calculated as:

$$q_v = \frac{p_{atm} \cdot (\Delta V / \Delta t)}{RT}, \tag{9}$$

where p_{atm} is the reference pressure in the flowmeter, T the temperature of the working volume and $R = 8.3145\ \mathrm{J \cdot mol^{-1} \cdot K^{-1}}$ the ideal gas constant. The whole calibration system and the leak is surrounded by a water bath of controlled temperature and carefully thermally insulated. Four calibrated Pt100 sensors are used to record the temperatures of the temperature-controlled water, the working and reference volume and the temperature close to the test leak under calibration.

Details of the system, the measurement procedure and the measurement uncertainties are given in [6].

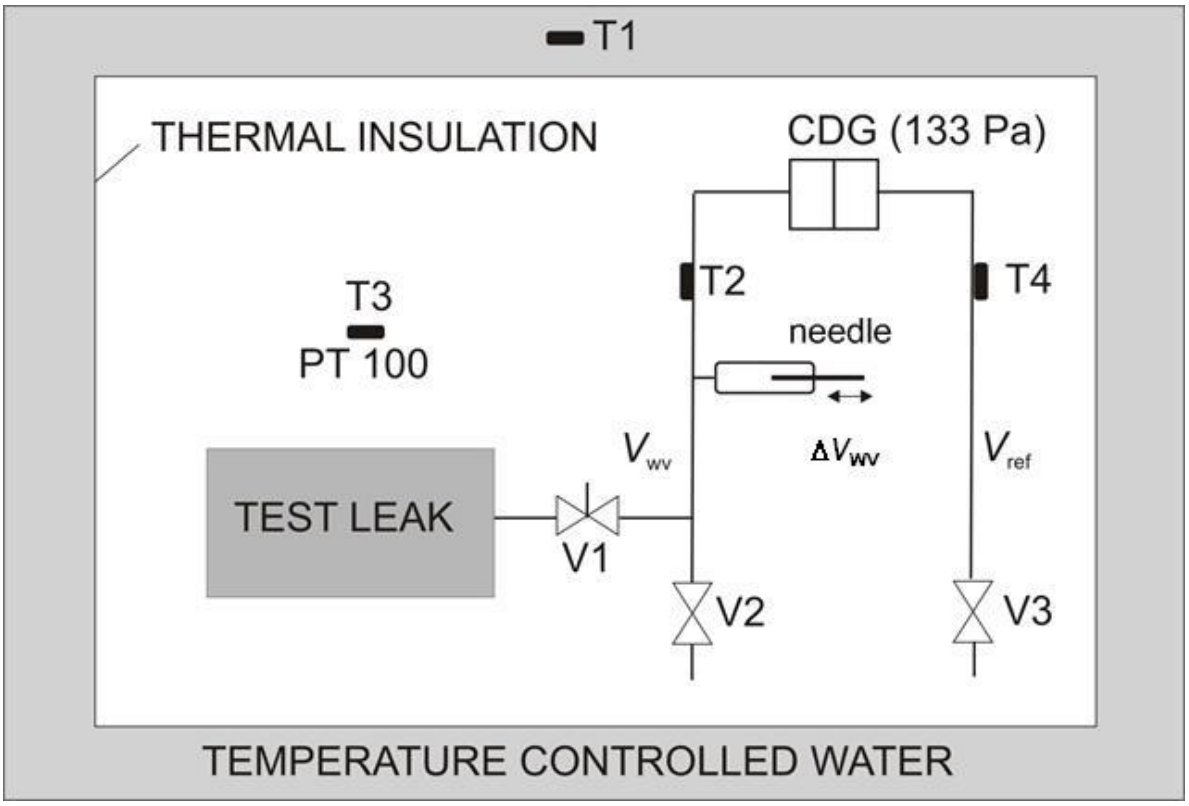

Figure 5. Scheme of the primary standard.

4. Chronology

In order to determine the stability over time of q_v, it was decided that the pilot laboratory will calibrate again the transfer standards at the end of the comparison. Each laboratory measured the flow rates from L1 and L2. No significant delays occurred during the comparison. Table 3 presents the actual chronology of the calibrations.

Table 3. Chronology of measurements for the comparison purpose. LNEx means the xth calibration sequence carried out by LNE, *x* being equal to 1 or 2. Date format: dd/mm/yyyy

Calibrating Laboratory	L1 1st measurement	L1 2nd measurement	L2 1st measurement	L2 2nd measurement
LNE1	21/10/2009 to 22/10/2009	29/10/2009 to 30/10/2009	24/10/2009 to 25/10/2009	04/11/2009 to 06/11/2009
PTB	28/12/2009	18/01/2010 to 19/01/2010	14/12/2009 to 15/12/2009	04/01/2010 to 05/01/2010
INRIM	25/01/2010 to 29/01/2010	17/02/2010 to 22/02/2010	01/02/2010 to 10/02/2010	24/02/2010 to 04/03/2010
CMI	27/03/2010	17/04/2010	04/04/2010	10/04/2010
LNE2	08/05/2010 to 09/05/2010	26/05/2010 to 27/05/2010	01/05/2010 to 03/05/2010	19/05/2010 to 21/05/2010

5. Measurement procedure

5.1. Transportation

To avoid any incident with transportation, the transfer standards were brought by each participant to the next one.

5.2. Installation

The connecting port of the leak was attached to each NMI's calibration system in a horizontal orientation, except when the PTB checked the influence of the orientation. The leaks were not connected to an oily or vacuum system and no valve was placed downstream of the leak. The leak was maintained one day at the temperature of (20.0 ± 0.30) °C before measurement. During the measurements, except for the CMI, the temperature of the leak was fixed at (20.0 ± 0.30) °C.

5.3. Calibration procedure

Each laboratory was required to perform ten measurements and to repeat this series the week after.

INRIM performed a series over more than four days. The CMI, LNE and the PTB performed one series over two days.

Some additional measurements were carried out by the PTB, in order to check the pressure influence on leak L1, the temperature influence on leak L2 and the influence of the leak orientation (vertical or horizontal).

6. Uncertainty of reference standards

Table 4 presents the relative standard Type B uncertainties for the different standards and leaks' measured values. Type A uncertainties are evaluated following the scatter of repeated measurements using methods described in Sec. 7.

Table 4. Relative Type B standard uncertainties of measured leak rates.

NMI	L1	L2
CMI (first measurement)	0.74 %	1.4 %
CMI (second measurement)	0.53 %	1.4%
INRIM	2.8 %	4.9 %
LNE	2.0 %	2.0 %
PTB	0.63 %	0.82 %

7. Influence quantities on the transfer standard leaks

The influence quantities on the flow rate of the leak artefact, introduced in Section 3, are the temperature θ and the downstream pressure p_d. The temperature coefficient α (at 20 °C) and the pressure coefficient β (at p_{d0}) were determined from LNE data. Some measurements of the flow rate at different downstream pressure were performed at PTB. The flow rate stability of both leaks over the comparison, as well as the short term stability is evaluated by the pilot laboratory.

7.1. Temperature coefficient of transfer standard leaks

Before initiating the comparison, the artefacts were calibrated at three temperature levels (15 °C, 20 °C and 25 °C) to determine their temperature coefficient α. Results obtained for the leak L2 are showing a linear trend of the flow rate with temperature. For the leak L1, the scattered results did not allow to determine a reliable temperature coefficient.

The temperature of the artefact was controlled by means of a thermostated bath, as explained in Section 3.3. Standard uncertainty on the leak temperature was estimated to be 0.15 °C.

7.1.1. Leak L2

Measurement results are plotted Figure 6.

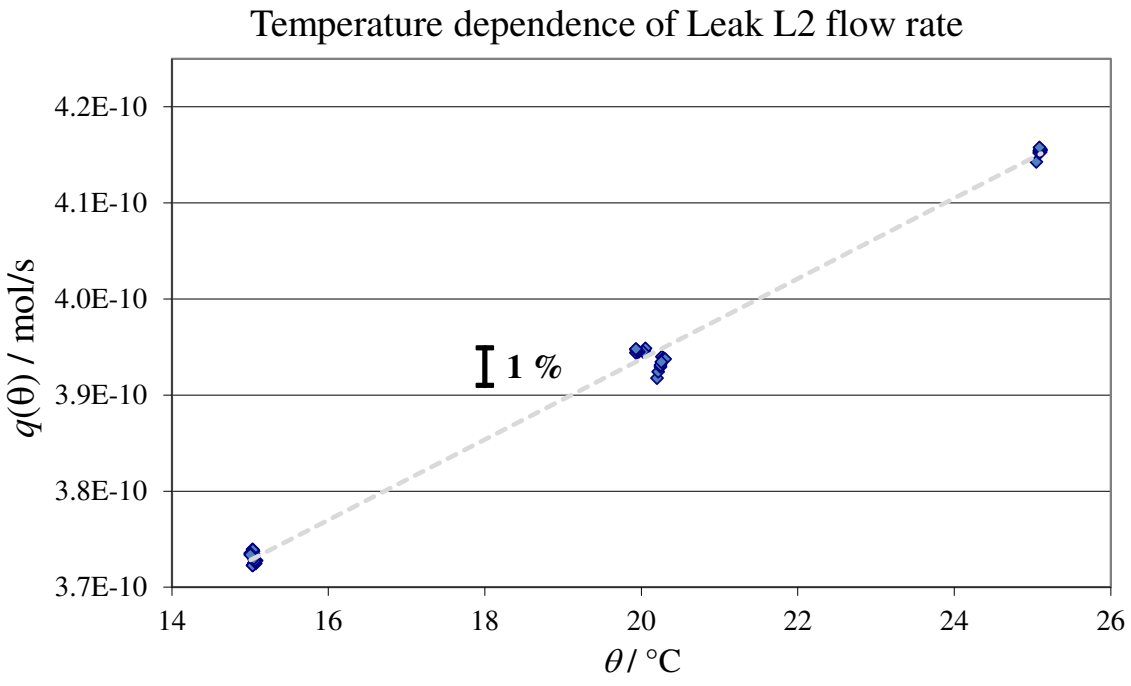

Figure 6. Plots of the measured flow rates versus temperature for the leak L2.

An ordinary linear least square fit was applied to the data to determine the slope α_{L2} as a function of temperature. $\alpha_{L2}\, u_{\alpha L2}$ is the corresponding standard deviation of the slope:

$$\alpha_{L2} = \alpha = (4.19 \pm 0.041) \cdot 10^{-12}\ \mathrm{mol \cdot s^{-1} \cdot {}^{\circ}C^{-1}}. \qquad (10)$$

which is about 1.1 % per °C, when normalized at 20 °C.

7.1.2. Leak L1

Flow rate measurements were performed at 15 °C, 20 °C and 25 °C (23 °C instead of 25 °C in the series after the comparison). Results obtained before the comparison are plotted in Figure 7.

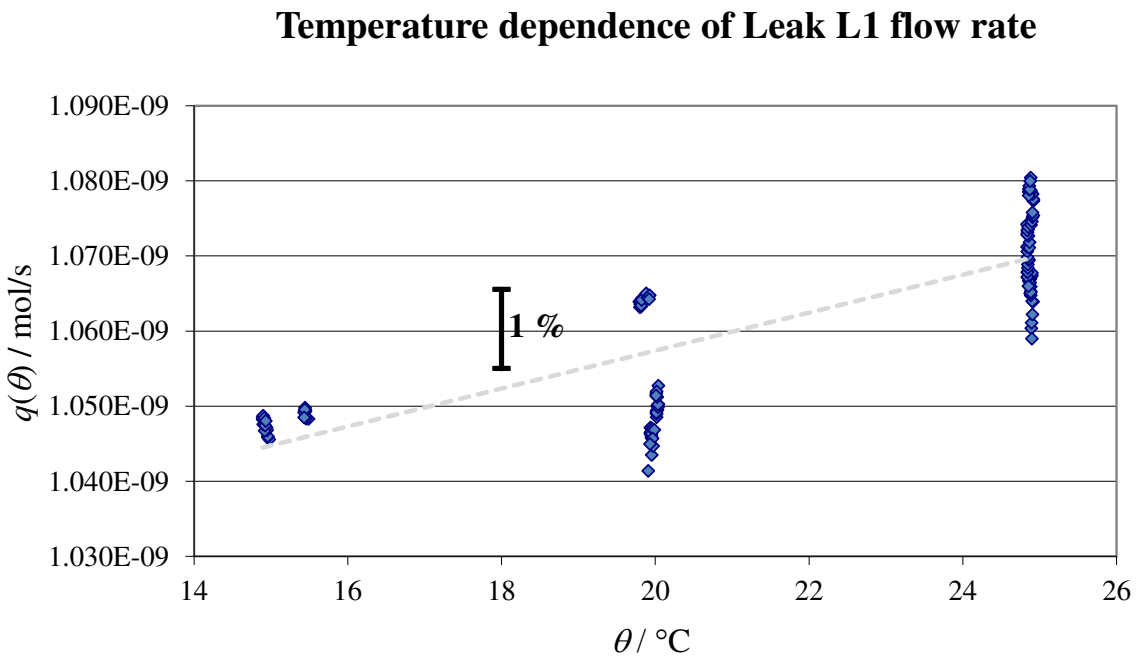

Figure 7. Plots of the measured flow rates versus temperature for the leak L1.

Scattered values of the L1 flow rates indicate an anomalous behaviour of the leak L1. Its metrological history (Section 7.3.2) confirms this observation.

7.2. Downstream pressure coefficient

With the LNE reference standard, it is not possible to adjust the downstream pressure p_d at a fixed value, to check the dependence of the leak artefact flow rate with p_d. During a measurement, p_d is related to the atmospheric pressure. Many calibrations of the leak artefacts performed before and after the comparison allowed to observe a trend in the behaviour of the flow rate with p_d. Given the behaviour of L1 during the temperature coefficient determination, only the measurements for the leak L2 are presented.

Measurement points of the leak flow rate calculated at 20 °C, $q(20°C ; p_d)$ for each calibration of the leak L2 are plotted versus downstream pressure p_d in Figure 8. It can be seen that when, by chance, the atmospheric pressure significantly changes (and consequently the downstream pressure) during one calibration (for example, the series depicted with crosses in Figure 8), the trend of $q(20°C ; p_d)$ seems to be linear with p_d.

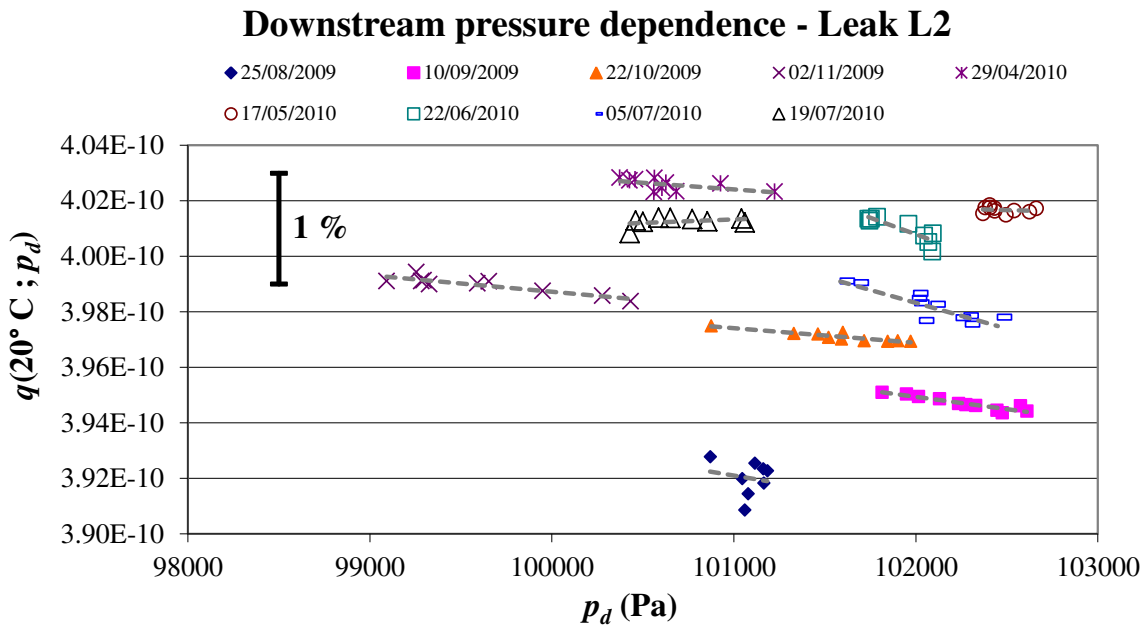

Figure 8. Measurement series of the leak L2 performed by the Pilot Laboratory versus downstream pressure; dashed lines are the linear regression for each series

A pressure coefficient β_{L2k} is thus calculated for each data set k with the ordinary least square method. Results are reported in Table 5. The standard uncertainty $u_{\beta L2k}$ is the standard deviation of the linear regression. The values of β_{L2k} and $u_{\beta L2k}$ are also given in % per kPa for a better clarity. The last column of Table 5 is the ratio $u_{\beta L2k}$ / β_{L2k} which allows to calculate the correlation coefficient ρ ($u_{\beta L2k}$ / β_{L2k} ; Δp_{dk}), where Δp_{dk} is the downstream pressure change during a calibration. ρ ($u_{\beta L2k}$ / β_{L2k} ; Δp_{dk})= – 0.7, which means that the larger the atmospheric pressure variation during a calibration is, the better the knowledge of β_{L2} is obtained.

From these considerations, the pressure coefficient β_{L2} is calculated as the mean of the β_{L2k} weighted by the inverse of $(u_{\beta L2k})^2$, from the series of the 22/10/2009 and 02/11/2009. The highest value of $u_{\beta L2k}$ on these series is selected as the uncertainty of $u_{\beta L2}$.

The pressure coefficient obtained for leak artefact L2 is:

$$\beta_{L2} = \beta = (-5.56 \pm 0.60) \cdot 10^{-16}\ \mathrm{mol \cdot s^{-1} \cdot Pa^{-1}}, \qquad (11)$$

Table 5. Pressure coefficients calculated on 9 measurement series with associated standard uncertainty

Date of measurement k	Δp_{dk} kPa	β_{L2k} mol·s^{-1}·Pa^{-1}	$u_{\beta L2k}$ mol·s^{-1}·Pa^{-1}	β_{L2k} % per kPa	$u_{\beta L2k}$ / Δp_{dk} % per kPa	$u_{\beta L2k}$ / β_{L2k} %
25/08/2009	0.314	-1.09E-15	2.5E-15	-0.28	0.63	228
10/09/2009	0.796	-8.96E-16	1.1E-16	-0.23	0.03	13
22/10/2009	1.096	-5.30E-16	7.9E-17	-0.13	0.02	15
02/11/2009	1.342	-5.97E-16	9.9E-17	-0.15	0.02	17
29/04/2010	0.851	-4.70E-16	2.4E-16	-0.12	0.06	50
17/05/2010	0.292	-1.79E-16	3.7E-16	-0.04	0.09	205
22/06/2010	0.355	-2.40E-15	5.1E-16	-0.59	0.13	21
05/07/2010	0.865	-1.86E-15	3.4E-16	-0.46	0.08	18
19/07/2010	0.634	2.56E-16	2.5E-16	0.06	0.06	98

From PTB measurements (three sets), the calculated pressure coefficient is:

$$\beta_{L2-PTB} = (-9.7 \pm 10) \cdot 10^{-15}\ \mathrm{mol \cdot s^{-1} \cdot Pa^{-1}}, \tag{12}$$

which is compatible with β_{L2}. However, considering the higher uncertainty of $\beta_{L2\text{-}PTB}$, the chosen pressure coefficient is that of Equation (11), which is about -0.14 % per kPa.

7.3. Time stability

In this section, the reported results are from LNE calibrations before, during and after the course of the comparison. The reference flow rate $q(\theta_0; p_{d0})$ at the temperature θ_0 and the downstream pressure p_{d0} (see section 2), is calculated from the measured flow rate $q(\theta; p_d)$ using the following formula:

$$q(\theta_0; p_{d0}) = q(\theta; p_d) + \alpha(\theta - \theta_0) + \beta(p_d - p_{d0}). \tag{13}$$

Common temperature and pressure coefficients α and β are assumed for both leaks L1 and L2 as they are of the same model and because it was not possible to calculate such coefficients for L1, due to its short-term instability.

To study the time dependence of an artefact, the uncertainty u' related to the measurement repeatability and the climatic conditions is used. It is the combination of the repeatability u_A and the uncertainty $u_{\theta,pd}$ calculated as follows:

$$u_{\theta,pd} = \sqrt{[\alpha \cdot u_\theta]^2 + [u_\alpha \cdot |\theta - \theta_0|]^2 + \left[\beta \cdot u_{pd}\right]^2 + \left[u_\beta \cdot |p_d - p_{d0}|\right]^2}, \tag{14}$$

where u_α and u_β are the uncertainties of the coefficients α and β (Equations (10) and (11)), u_θ and u_{pd} are the uncertainties of the temperature and the downstream pressure determination during a measurement.

Finally:

$$u' = \sqrt{{u_A}^2 + {u_{\theta,pd}}^2}. \quad (15)$$

7.3.1. Leak L2

Figure 9 shows the successive flow rates of L2 determined between 05/06/2009 and 19/07/2010. As one can see from the five last measurements in this figure, there is some instability on the short-term of the leak L2. An uncertainty contribution u_{L2} (roughly in the order of magnitude of 1 % from the graph) can then be attributed to this transfer standard.

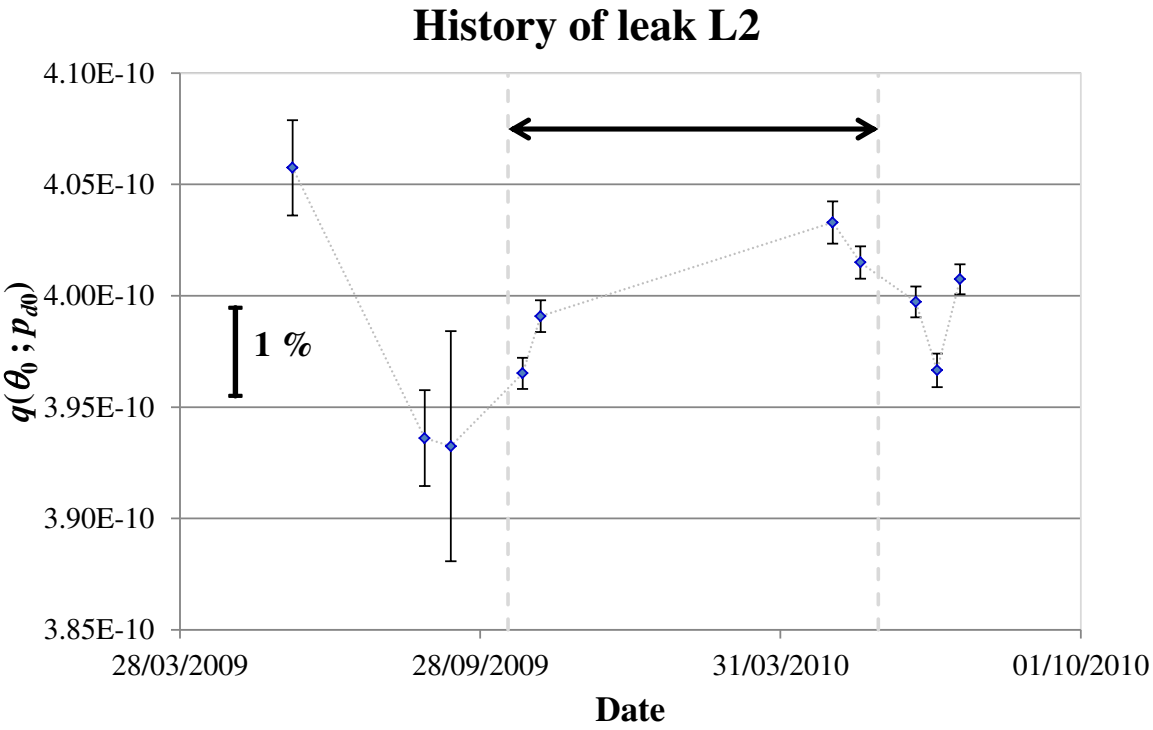

Figure 9. Measurement series of the leak L2 performed by the pilot laboratory. The horizontal arrow delimitates the period of the comparison. Vertical bars represent uncertainty *u'*.

7.3.2. Leak L1

Similarly to leak L2, Figure 10 shows the successive determined flow rates of L1 between 04/06/2009 and 28/07/2010. The instability is much larger than that observed for L2. The maximum deviation among the leak rate values is about 17 %. As a conclusion, the leak L1 is not suitable to demonstrate the capabilities of the participants (Table 4). The measurements performed with the leak L1 are then not reported nor analysed in the report.

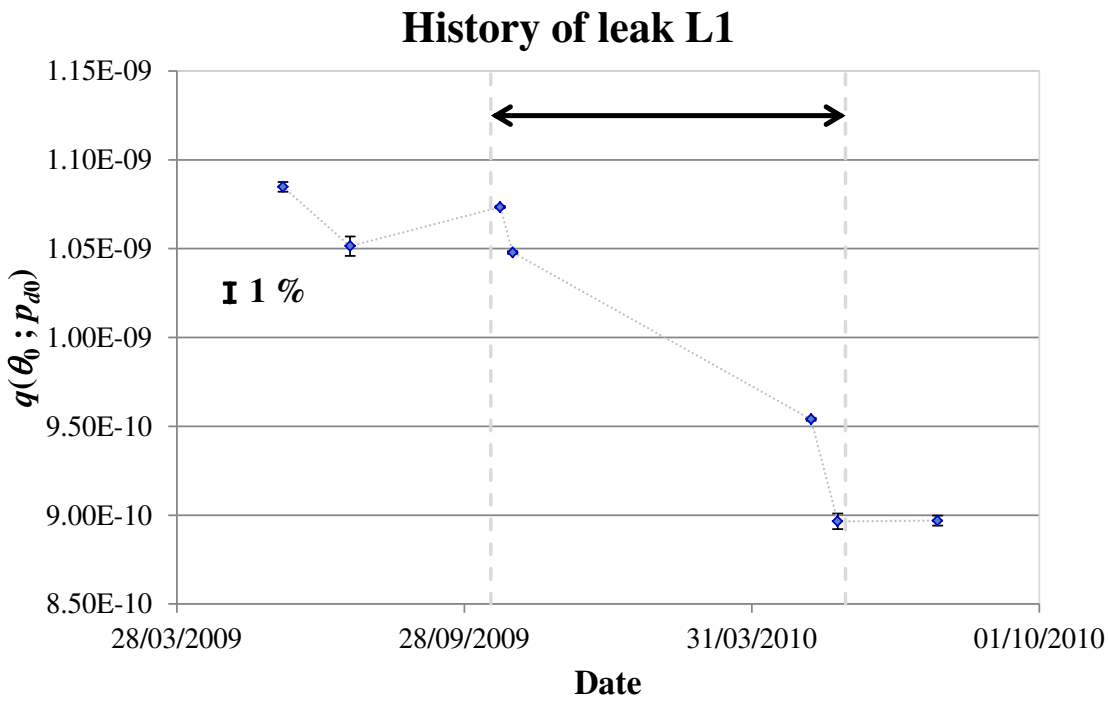

Figure 10. Measurement series of the leak L1 performed by the pilot laboratory. The horizontal arrow delimitates the period of the comparison. Vertical bars represent *u'*.

7.4. Influence of the orientation of the leak artefacts

A horizontal orientation of the leak was required during the calibration. However, in the case of the CMI calibration, it was not possible to fulfil this requirement (leak is installed in a vertical orientation on the CMI's standard). To check the influence of the orientation, PTB has performed some additional measurements with the leak artefacts installed in a vertical position. It was concluded that orientation of transfer standards does not significantly affect the leak flow rate.

8. Results of the pilot laboratory

8.1. Reporting the results

Table shows the results obtained by the pilot laboratory. LNE1 and LNE2 is the calibration at the start of the comparison and at the end of the comparison respectively. The latter is used to estimate the stability of the leak artefact over the course of the comparison. Successive measurement sequences are denoted **a** and **b**.

Table 6. Results of the pilot laboratory for L2. $q(\theta; p_d)$ is the leak molar flow rate at the temperature θ and the downstream pressure p_d of the leak at the time of the calibration. u_B is the type B standard uncertainty ($k = 1$).

NMI	Date	$q(\theta; p_d)$	u_B	p_d	u_{pd}	θ	u_θ
		mol/s	mol/s	Pa	Pa	°C	°C
LNE 1a	24/10/2009	3.9770E-10	8.0E-12	100875	38	20.05	0.15
	24/10/2009	3.9741E-10	7.9E-12	101329	48	20.04	0.15
	24/10/2009	3.9730E-10	7.9E-12	101519	43	20.05	0.15
	24/10/2009	3.9733E-10	7.9E-12	101462	28	20.03	0.15
	24/10/2009	3.9713E-10	7.9E-12	101591	39	20.02	0.15
	25/10/2009	3.9739E-10	7.9E-12	101599	39	20.03	0.15
	25/10/2009	3.9718E-10	7.9E-12	101716	41	20.05	0.15
	25/10/2009	3.9710E-10	7.9E-12	101844	30	20.04	0.15
	25/10/2009	3.9705E-10	7.9E-12	101900	26	20.02	0.15
	25/10/2009	3.9693E-10	7.9E-12	101971	28	20.00	0.15
LNE 1b	4/11/2009	3.9909E-10	8.0E-12	99091	44	20.00	0.15
	4/11/2009	3.9929E-10	8.0E-12	99326	53	20.07	0.15
	4/11/2009	3.9892E-10	8.0E-12	99282	16	19.96	0.15
	4/11/2009	3.9860E-10	8.0E-12	99294	19	19.88	0.15
	4/11/2009	3.9888E-10	8.0E-12	99255	32	19.88	0.15
	5/11/2009	3.9902E-10	8.0E-12	99590	51	20.00	0.15
	5/11/2009	3.9941E-10	8.0E-12	99654	52	20.07	0.15
	5/11/2009	3.9892E-10	8.0E-12	99949	14	20.04	0.15
	5/11/2009	3.9854E-10	8.0E-12	100278	15	19.99	0.15
	6/11/2009	3.9842E-10	8.0E-12	100433	60	20.01	0.15
LNE 2a	1/05/2010	4.0305E-10	8.1E-12	100684	36	20.15	0.15
	1/05/2010	4.0318E-10	8.1E-12	100604	43	20.16	0.15
	2/05/2010	4.0285E-10	8.1E-12	100560	46	20.12	0.15
	2/05/2010	4.0332E-10	8.1E-12	100426	61	20.13	0.15
	2/05/2010	4.0343E-10	8.1E-12	100457	29	20.14	0.15
	2/05/2010	4.0356E-10	8.1E-12	100373	63	20.16	0.15
	3/05/2010	4.0347E-10	8.1E-12	100563	42	20.14	0.15
	3/05/2010	4.0345E-10	8.1E-12	100627	68	20.17	0.15
	3/05/2010	4.0343E-10	8.1E-12	100927	34	20.18	0.15
	3/05/2010	4.0319E-10	8.1E-12	101224	54	20.19	0.15
LNE 2b	19/05/2010	4.0148E-10	8.0E-12	102369	45	19.99	0.15
	19/05/2010	4.0155E-10	8.0E-12	102434	27	19.98	0.15
	19/05/2010	4.0157E-10	8.0E-12	102382	37	19.96	0.15
	19/05/2010	4.0159E-10	8.0E-12	102408	41	19.96	0.15
	20/05/2010	4.0147E-10	8.0E-12	102540	36	19.96	0.15
	20/05/2010	4.0160E-10	8.0E-12	102661	35	19.97	0.15
	20/05/2010	4.0144E-10	8.0E-12	102625	32	19.96	0.15
	20/05/2010	4.0160E-10	8.0E-12	102406	33	19.95	0.15
	21/05/2010	4.0143E-10	8.0E-12	102432	35	19.93	0.15
	21/05/2010	4.0123E-10	8.0E-12	102496	52	19.94	0.15

8.2. Reducing the data

A first data reduction is made in Table with the calculation of $q(\theta_0; p_{d0})$ and $u_{\theta,pd}$ using Equations (13) and (14).

Table 7. Results of the pilot laboratory for L2. $q(\theta_0; p_{d0})$ is the leak flow rate at 20 °C and 100000 Pa. $u_{\theta,pd}$ is the contribution in uncertainty of the temperature and the downstream pressure (k=1).

NMI	Date	Time	$q(\theta_0; p_{d0})$	u_B	$u_{\theta,pd}$
		HH:MM	mol/s	mol/s	mol/s
LNE 1a	24/10/2009	18:43	3.9741E-10	8.0E-12	6.6E-13
	24/10/2009	4:27	3.9685E-10	7.9E-12	6.6E-13
	24/10/2009	9:48	3.9666E-10	7.9E-12	6.7E-13
	24/10/2009	15:10	3.9663E-10	7.9E-12	6.5E-13
	24/10/2009	20:33	3.9635E-10	7.9E-12	6.4E-13
	25/10/2009	1:55	3.9663E-10	7.9E-12	6.5E-13
	25/10/2009	7:18	3.9643E-10	7.9E-12	6.7E-13
	25/10/2009	12:41	3.9623E-10	7.9E-12	6.6E-13
	25/10/2009	18:06	3.9608E-10	7.9E-12	6.4E-13
	25/10/2009	23:30	3.9583E-10	7.9E-12	6.4E-13
LNE 1b	04/11/2009	0:24	3.9959E-10	8.0E-12	6.3E-13
	04/11/2009	5:42	3.9995E-10	8.0E-12	6.9E-13
	04/11/2009	11:01	3.9917E-10	8.0E-12	6.5E-13
	04/11/2009	16:21	3.9850E-10	8.0E-12	8.0E-13
	04/11/2009	21:40	3.9880E-10	8.0E-12	8.0E-13
	05/11/2009	3:00	3.9925E-10	8.0E-12	6.3E-13
	05/11/2009	8:20	3.9990E-10	8.0E-12	7.0E-13
	05/11/2009	13:40	3.9911E-10	8.0E-12	6.5E-13
	05/11/2009	19:01	3.9834E-10	8.0E-12	6.3E-13
	06/11/2009	0:22	3.9823E-10	8.0E-12	6.3E-13
LNE 2a	01/05/2010	16:36	4.0332E-10	8.1E-12	9.0E-13
	01/05/2010	22:09	4.0352E-10	8.1E-12	9.2E-13
	02/05/2010	3:23	4.0303E-10	8.1E-12	8.0E-13
	02/05/2010	8:39	4.0362E-10	8.1E-12	8.3E-13
	02/05/2010	13:52	4.0379E-10	8.1E-12	8.7E-13
	02/05/2010	19:07	4.0402E-10	8.1E-12	9.2E-13
	03/05/2010	0:18	4.0376E-10	8.1E-12	8.7E-13
	03/05/2010	5:32	4.0382E-10	8.1E-12	9.6E-13
	03/05/2010	10:44	4.0366E-10	8.1E-12	9.8E-13
	03/05/2010	15:59	4.0329E-10	8.1E-12	1.0E-12
LNE 2b	19/05/2010	5:32	4.0010E-10	8.0E-12	6.5E-13
	19/05/2010	10:50	4.0012E-10	8.0E-12	6.5E-13
	19/05/2010	16:09	4.0007E-10	8.0E-12	6.7E-13
	19/05/2010	21:28	4.0010E-10	8.0E-12	6.6E-13
	20/05/2010	2:46	3.9989E-10	8.0E-12	6.7E-13
	20/05/2010	8:04	4.0000E-10	8.0E-12	6.6E-13
	20/05/2010	13:22	3.9982E-10	8.0E-12	6.7E-13
	20/05/2010	18:43	4.0004E-10	8.0E-12	6.8E-13
	21/05/2010	0:00	3.9980E-10	8.0E-12	7.0E-13
	21/05/2010	5:22	3.9960E-10	8.0E-12	6.9E-13

The second reduction in Table consists in taking the mean of the measurements $\bar{q}(\theta_0; p_{d0})$ in each sequence *a* and *b* for calibration LNE1 and LNE2. The repeatability is given by the standard deviation of the mean:

$$u_A = \sqrt{\frac{1}{(N-1)}\sum_{i=1}^{N}\left[q_i\left(\theta_0; p_{d0}\right) - \bar{q}\left(\theta_0; p_{d0}\right)\right]^2}, \tag{16}$$

with *i* the index of a single measurement in a sequence, and *N* the number of measurements.

Uncertainty corresponding to type B evaluation u'_B takes into account the contribution of the calibration temperature and the downstream pressure of the leak artefact $u_{\theta,pd}$:

$$u'_B = \sqrt{u_B^2 + \left(u_{\theta,pd}\right)^2}, \tag{17}$$

Table 8. Mean results of the pilot laboratory for L2 for each sequence **a** and **b**. u_A is the standard deviation of the mean.

NMI	Date	$q(\theta_0; p_{d0})$	u_A	u'_B
		mol/s	mol/s	mol/s
LNE 1a	24/10/2009	3.9651E-10	1.4E-13	7.9E-12
LNE 1b	04/11/2009	3.9908E-10	2.0E-13	8.0E-12
LNE 2a	02/05/2010	4.0329E-10	9.4E-14	8.1E-12
LNE 2b	19/05/2010	4.0149E-10	5.5E-14	8.0E-12

Results of two consecutive sequences are considered compatible if:

$$\left|q_a\left(\theta_0; p_{d0}\right) - q_b\left(\theta_0; p_{d0}\right)\right| \leq \sqrt{u_{A,a}^2 + u_{A,b}^2}. \tag{18}$$

Index *a* and *b* are used to denote the sequences **a** and **b**.

For both calibrations LNE1 and LNE 2, results violate condition (18). To further reduce the results, the uncertainty associated to the mean of all the measurements of sequence **a** and sequence **b** is the quadratic combination of the repeatability u_A (which is the standard deviation of the mean), u'_B and the half difference of $|q_a(\theta_0; p_{d0}) - q_b(\theta_0; p_{d0})|$. Results are shown in Table .

Table 9. Mean results of the pilot laboratory for L2 at the start and at the end of the comparison.

NMI	Date	$q(\theta_0; p_{d0})$	u
		mol/s	mol/s
LNE 1	24/10/2009	3.978E-10	8.1E-12
LNE 2	02/05/2010	4.024E-10	8.1E-12

An uncertainty contribution $u_{drift,L2}$ due to the leak's drift is estimated from the difference between the two calibrations performed by the pilot laboratory, on which a rectangular distribution is associated. Consequently:

$$u_{drift,L2} = 2.7 \times 10^{-12}\ \mathrm{mol \cdot s^{-1}}, \quad (19)$$

that is 0.67 % in relative value.

This value is significantly high regarding the calibration uncertainty reported by PTB (Table 4) as they are of the same order of magnitude but can be considered sufficiently low to demonstrate the capabilities of CMI and LNE.

9. Reported results of each laboratory

Table 10. Reported results by PTB and CMI for leak L2.

NMI	Date	$q(\theta; p_d)$	u_B	p_d	u_{pd}	θ	u_θ
		mol/s	mol/s	Pa	Pa	°C	°C
PTBa	14/12/2009	3.9962E-10	3.2E-12	101770	102	20.36	0.10
	14/12/2009	4.0131E-10	3.2E-12	101749	102	20.32	0.10
	15/12/2009	3.9520E-10	3.2E-12	101625	102	20.16	0.10
	15/12/2009	3.9989E-10	3.3E-12	101640	102	20.17	0.10
	15/12/2009	4.0054E-10	3.3E-12	101642	102	20.18	0.10
	15/12/2009	4.0109E-10	3.3E-12	101652	102	20.18	0.10
	15/12/2009	3.9815E-10	3.3E-12	101651	102	20.18	0.10
	15/12/2009	4.0188E-10	3.3E-12	101657	102	20.18	0.10
	15/12/2009	4.0546E-10	3.3E-12	101656	102	20.18	0.10
	15/12/2009	4.0413E-10	3.3E-12	101649	102	20.20	0.10
PTBb	04/01/2010	3.9546E-10	3.3E-12	101188	101	20.01	0.10
	04/01/2010	4.0247E-10	3.3E-12	101061	101	20.01	0.10
	04/01/2010	3.9808E-10	3.3E-12	101040	101	20.01	0.10
	04/01/2010	4.0429E-10	3.3E-12	101010	101	20.01	0.10
	04/01/2010	4.0665E-10	3.3E-12	101011	101	20.01	0.10
	04/01/2010	4.0045E-10	3.3E-12	100995	101	20.01	0.10
	04/01/2010	3.7839E-10	3.1E-12	100991	101	20.01	0.10
	05/01/2010	4.0358E-10	3.3E-12	100490	100	20.00	0.10
	05/01/2010	4.0915E-10	3.4E-12	100478	100	20.00	0.10
	05/01/2010	4.1428E-10	3.4E-12	100461	100	20.01	0.10
CMIa	04/04/2010	4.1380E-10	6.0E-12	97900	600	20.01	0.15
	04/04/2010	4.0240E-10	6.0E-12	97900	600	20.01	0.15
	04/04/2010	4.0630E-10	6.0E-12	97900	600	20.01	0.15
	04/04/2010	4.0920E-10	6.0E-12	97900	600	20.01	0.15
	04/04/2010	4.1450E-10	6.0E-12	97900	600	20.01	0.15
	04/04/2010	4.1610E-10	6.0E-12	97900	600	20.01	0.15
	04/04/2010	4.2060E-10	6.0E-12	97900	600	20.01	0.15
	04/04/2010	4.1430E-10	6.0E-12	97900	600	20.01	0.15
	04/04/2010	4.1440E-10	6.0E-12	97900	600	20.01	0.15
	04/04/2010	4.1350E-10	6.0E-12	97900	600	20.01	0.15
CMIb	10/04/2010	4.0480E-10	5.5E-12	98800	600	20.07	0.18
	10/04/2010	4.0990E-10	5.5E-12	98800	600	20.07	0.18
	10/04/2010	4.0720E-10	5.5E-12	98800	600	20.07	0.18
	10/04/2010	4.1390E-10	5.5E-12	98800	600	20.07	0.18
	10/04/2010	4.2660E-10	5.5E-12	98800	600	20.07	0.18
	10/04/2010	4.0080E-10	5.5E-12	98800	600	20.07	0.18
	10/04/2010	4.2080E-10	5.5E-12	98800	600	20.07	0.18
	10/04/2010	4.1440E-10	5.5E-12	98800	600	20.07	0.18
	10/04/2010	4.0390E-10	5.5E-12	98800	600	20.07	0.18
	10/04/2010	4.0640E-10	5.5E-12	98800	600	20.07	0.18

Results of CMI and PTB are presented the same way it was done for the pilot laboratory. Table shows the results as they were reported by the laboratories. Then data are reduced with the calculation of $q(\theta_0; p_{d0})$ in Table 5.

Table 5. Results of the pilot laboratory for L2. $q(\theta_0; p_{d0})$ is the leak flow rate at 20 °C and 100000 Pa. $u_{\theta,pd}$ is the contribution in uncertainty of the temperature and the downstream pressure (k=1).

NMI	Date	$q(\theta_0; p_{d0})$	u_B	$u_{\theta,pd}$
		mol/s	mol/s	mol/s
PTBa	14/12/2009	4.0014E-10	1.8E-13	1.6E-12
	14/12/2009	4.0168E-10	1.8E-13	1.4E-12
	15/12/2009	3.9497E-10	1.7E-13	8.0E-13
	15/12/2009	3.9969E-10	1.7E-13	8.3E-13
	15/12/2009	4.0038E-10	1.7E-13	8.7E-13
	15/12/2009	4.0093E-10	1.7E-13	8.7E-13
	15/12/2009	3.9799E-10	1.7E-13	8.7E-13
	15/12/2009	4.0171E-10	1.7E-13	8.7E-13
	15/12/2009	4.0530E-10	1.7E-13	8.7E-13
	15/12/2009	4.0405E-10	1.7E-13	9.4E-13
PTBb	04/01/2010	3.9485E-10	1.3E-13	4.3E-13
	04/01/2010	4.0192E-10	1.2E-13	4.3E-13
	04/01/2010	3.9754E-10	1.2E-13	4.3E-13
	04/01/2010	4.0377E-10	1.1E-13	4.3E-13
	04/01/2010	4.0613E-10	1.1E-13	4.3E-13
	04/01/2010	3.9994E-10	1.1E-13	4.3E-13
	04/01/2010	3.7788E-10	1.1E-13	4.3E-13
	05/01/2010	4.0331E-10	7.4E-14	4.2E-13
	05/01/2010	4.0889E-10	7.3E-14	4.2E-13
	05/01/2010	4.1407E-10	7.2E-14	4.3E-13
CMIa	04/04/2010	4.1501E-10	3.9E-13	7.2E-13
	04/04/2010	4.0361E-10	3.9E-13	7.2E-13
	04/04/2010	4.0751E-10	3.9E-13	7.2E-13
	04/04/2010	4.1041E-10	3.9E-13	7.2E-13
	04/04/2010	4.1571E-10	3.9E-13	7.2E-13
	04/04/2010	4.1731E-10	3.9E-13	7.2E-13
	04/04/2010	4.2181E-10	3.9E-13	7.2E-13
	04/04/2010	4.1551E-10	3.9E-13	7.2E-13
	04/04/2010	4.1561E-10	3.9E-13	7.2E-13
	04/04/2010	4.1471E-10	3.9E-13	7.2E-13
CMIb	10/04/2010	4.0576E-10	3.5E-13	8.8E-13
	10/04/2010	4.1086E-10	3.5E-13	8.8E-13
	10/04/2010	4.0816E-10	3.5E-13	8.8E-13
	10/04/2010	4.1486E-10	3.5E-13	8.8E-13
	10/04/2010	4.2756E-10	3.5E-13	8.8E-13
	10/04/2010	4.0176E-10	3.5E-13	8.8E-13
	10/04/2010	4.2176E-10	3.5E-13	8.8E-13
	10/04/2010	4.1536E-10	3.5E-13	8.8E-13
	10/04/2010	4.0486E-10	3.5E-13	8.8E-13
	10/04/2010	4.0736E-10	3.5E-13	8.8E-13

Mean values are calculated for each sequence **a** and **b** in Table 6 and the consistency of these values is checked regarding the repeatability, using condition (18).

Table 6. Mean results of CMI and PTB for L2 for each sequence **a** and **b**. u_A is the standard deviation of the mean.

NMI	Date	$q(\theta_0; p_{d0})$	u_A	u'_B
		mol/s	mol/s	mol/s
PTBa	15/12/2009	4.0068E-10	9.2E-13	3.5E-12
PTBb	04/01/2010	4.0083E-10	3.1E-12	4.5E-12
CMIa	04/04/2010	4.1372E-10	1.6E-12	6.3E-12
CMIb	10/04/2010	4.1183E-10	2.6E-12	6.1E-12

Contrary to the pilot laboratory, the mean values in each sequence **a** and **b** are compatible, for CMI and PTB. However, one can observe that the repeatability within a single sequence of LNE is roughly ten times better than that of CMI and PTB. But the large difference obtained between measurement sequences **a** and **b**, regarding this small repeatability, has led to take into account a supplementary uncertainty component (§ 8.2). This latter combined to LNE repeatability finally lead to an uncertainty due to random effects approximately equal to CMI and PTB repeatability u_A.

In Table 7, the uncertainty of the laboratory is the quadratic combination of the repeatability u_A (which is the standard deviation of the mean) and u'_B.

Table 7. Mean results of PTB and CMI in the comparison.

NMI	Date	$q(\theta_0; p_{d0})$	u
		mol/s	mol/s
PTB	15/12/2009	4.008E-10	3.6E-12
CMI	04/04/2010	4.128E-10	6.2E-12

10. Illustration of the comparison results

Figure 11 illustrates the results obtained by the participants over the course of the comparison from Table and Table 7.

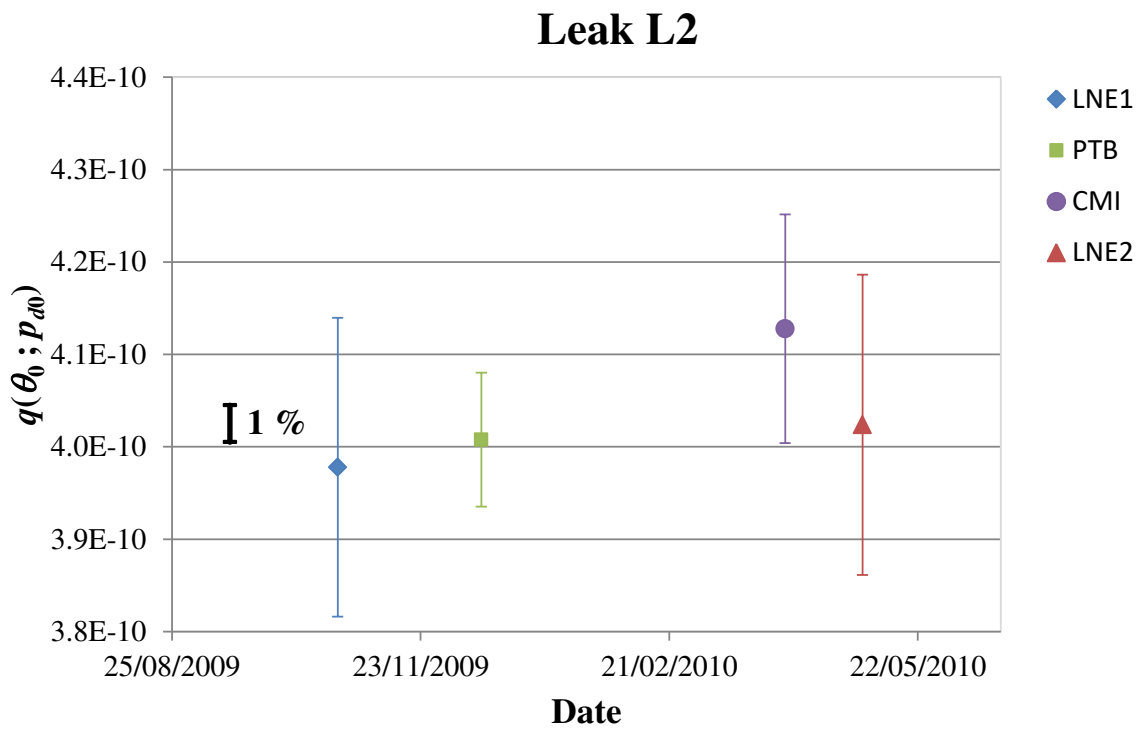

Figure 11. Results of the participants over the comparison. Vertical bars are the associated calibration uncertainties (k = 2)

One could consider a linear trend from the results of the pilot laboratory, however it was formerly shown that this hypothesis could not be demonstrated from the observation of the history graph of the leak L2 (Figure 9).

11. Reference value

11.1. Results summary

Table 8 sums-up the results of each laboratory j used to determine the reference value. For LNE, the first results identified by LNE1 were selected.

Table 8. Comparison results for the reference value determination.

NMI	$q_j(\theta_0;p_{d0})$ mol/s	u_j mol/s
LNE	3.978E-10	8.1E-12
PTB	4.008E-10	3.6E-12
CMI	4.128E-10	6.2E-12

11.2. Evaluation of the reference value

The reference leak flow rate $q_{ref}(\theta_0; p_{d0})$ is determined using the "Procedure B" described in [7]. It is the mean value of each Laboratory j ($j = 1$ to 3) $q_j(\theta_0; p_{d0})$ weighted by the inverse of the variance u_j^2:

$$q_{ref}(\theta_0; p_{d0}) = \sum_j \left(\frac{q_j / u_j^2}{\sum_j 1 / u_j^2} \right) = 4.030 \times 10^{-10} \text{ mol} \cdot \text{s}^{-1}. \quad (20)$$

The results consistency check consists in applying the chi-square test by calculating the parameter χ^2_{obs}:

$$\chi^2_{obs} = \sum_j \frac{(q_j - q_{ref})^2}{u_j^2}, \quad (21)$$

and comparing it to the value of the chi-square distribution with $(j - 1) = 2$ degrees of freedom at the probability of 0.05. That means the results are consistent if:

$$\chi^2_{obs} < 6.0. \quad (22)$$

In this comparison:

$$\chi^2_{obs} = 3.3. \quad (23)$$

Thus, the results are consistent.

The uncertainty of the reference value $u(q_{ref})$ is given by the following formula:

$$u(q_{ref}) = \left[\sum_j \frac{1}{u_j^2} \right]^{-1/2}. \quad (24)$$

$$u(q_{ref}) = 2.9 \times 10^{-12} \text{ mol} \cdot \text{s}^{-1}. \quad (25)$$

12. Comparison results and degree of equivalence

12.1. Deviation D_j from the reference value and associated uncertainty $u(D_j)$

The deviation of each participant result from the reference value is:

$$D_j = q(\theta_0; p_{d0}) - q_{ref}(\theta_0; p_{d0}). \quad (26)$$

The uncertainty of this deviation is the square root of the difference between the square of u_j and the square of $u(q_{ref})$ [7]. The uncertainty attributed to the transfer standard (Equation (19)) shall be also considered and so:

$$u(D_j) = \sqrt{[u_j]^2 - [u(q_{ref})]^2 + [u_{drift,L2}]^2}. \quad (27)$$

12.2. Final results with degree of equivalence E_j

The degree of equivalence E_j of one participant is given by the expression:

$$E_j = \frac{D_j}{u_j}. \quad (28)$$

The final results of the comparison $q_j(\theta_0; p_{d0})$, D_j and $U(D_j)$ (for $k = 2$) are presented in Table 9 and shown in Figure 12.

Table 9. Final results of the comparison: mean flow rate $q_j(\theta_0; p_{d0})$ measured by each participant, deviation D_j of this flow rate from the reference value and associated expanded uncertainty $U(D_j)$, and the degree of equivalence E_j.

NMI	$q_j(\theta_0; p_{d0})$ mol/s	D_j mol/s	$U(D_j)$ mol/s	E_j
LNE	3.978E-10	- 5.2E-12	1.6E-11	- 0.33
PTB	4.008E-10	- 2.3E-12	6.9E-12	- 0.33
CMI	4.128E-10	+ 9.7E-12	1.2E-11	+ 0.80

$|E_j| < 1$ in all cases. The participants demonstrated the equivalence of their results to the reference value.

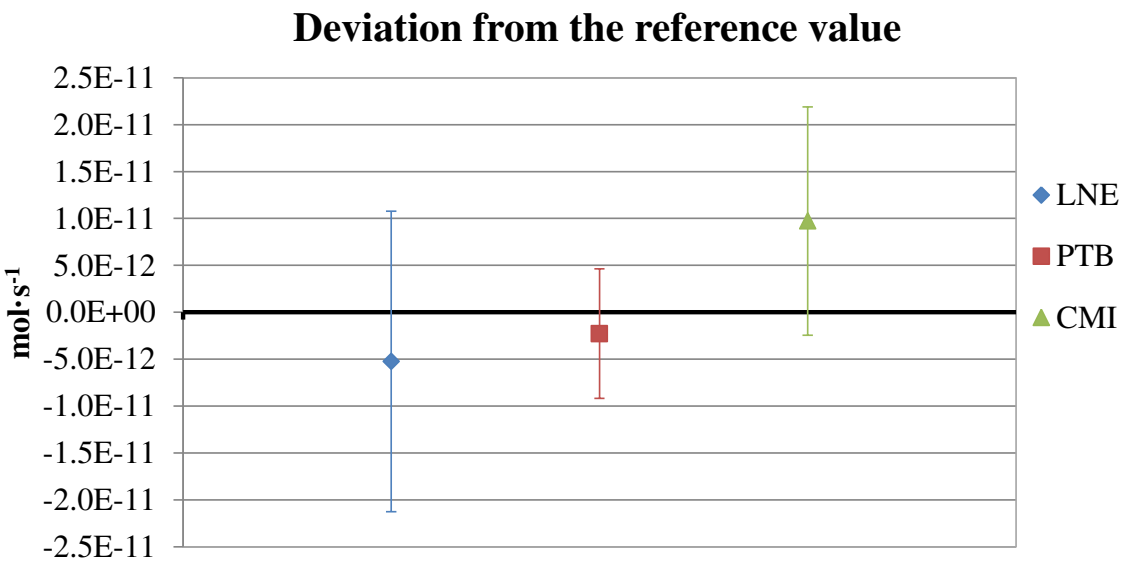

Figure 12. Comparison results of each participant; Vertical bars represent expanded uncertainties $U(D_j)$.

13. Conclusion

It was the first time that NMIs performed a comparison of small leak flow rates around $4 \cdot 10^{-10}$ mol/s flowing to atmosphere. It was done in the particular case of the cooling agent R-134a which remains (the comparison was carried out in 2009-2010) the reference gas in the standard EN 14624, which was amended in 2012. The latter gives directions to evaluate the performance of refrigerant leak detectors. The four participants were CMI, INRIM, LNE (pilot laboratory) and PTB. INRIM wished to withdraw its results considering that its uncertainty was too large at the time they perform the comparison. The three other participants used three different methods, all primary, which successfully gave measurements equivalent to the reference value. The artefacts were reservoir leaks of the same model provided by the pilot laboratory, which behaviour cannot be considered analogous to that of a pure gas leak. They actually contain R-134a in liquid and gaseous phase equilibrated at the saturation vapour pressure which is constant provided the temperature is also constant. On the two leak artefacts, one failed at giving a satisfying stability regarding the participants' calibration uncertainty. The second leak artefact has shown a better stability during the study, allowing the comparison of the results. The attributed uncertainty due to its drift is of the same order of magnitude as the calibration uncertainty of PTB and less than half the ones of CMI and LNE. An influence on the leak rate of the temperature ($\sim 1\ \% \cdot K^{-1}$) and to a less extent of the downstream pressure ($\sim -0.14\ \% \cdot kPa^{-1}$) were stated. Uncertainty due to these parameters was minimized by controlling and/or monitoring them and so was kept negligible regarding each laboratory's calibration uncertainty. In conclusion, such artefact is suitable to demonstrate measurement capabilities higher than about 1 % in relative value, provided that the lack of stability observed for one of the artefacts does not occur.

14. References

[1] K. Jousten *et al.*, 'Final report of key comparison CCM.P-K12 for very low helium flow rates (leak rates)', Metrologia, vol. 50, no. 1A, p. 07001, 2013.

[2] D. Pražák, J. Zuda and L.Peksa 'Calibration of secondary standard leaks by means of mass comparison. In: Proceedings of IMEKO 2010 TC3, TC5 and TC22 Conferences – Metrology in Modern Context' – November 22-25, 2010, Pattaya, Chonburi, Thailand. Thailand, 2010, p. 73-76.

[3] D. Pražák, J. Zůda, J. Tesař, L. Peksa, and M. Vičar, "Perspectives of atmospheric reference leaks calibration by gravimetric method," Measurement, vol. 46, no. 1, pp. 621–627, Jan. 2013.

[4] D. Pražák, L. Peksa, J. Tesař, T. Gronych, and M. Vičar, "A survey of the principles for primary standards for atmospheric halogenated-hydrocarbon-leaks," Metrologia, vol. 52, no. 4, p. R11, Apr. 2015.

[5] I. Morgado, J.-C. Legras and D. Clodic, ‘Primary standard for the calibration of refrigerant leak flow rates’, Metrologia, vol. 47, no. 3, pp. 135–145, 2010.
[6] K. Jousten and U. Becker, ‘A primary standard for the calibration of sniffer test leak devices’, Metrologia, vol. 46, no. 5, pp. 560–568, Oct. 2009.
[7] M. G. Cox, ‘The evaluation of key comparison data’, Metrologia, vol. 39, no. 6, p. 589, 2002.